Supplementary Information for

Intermolecular Headgroup Interaction and Hydration as Driving Forces for Lipid Transmembrane Asymmetry

Nikolay Smolentsev[a], Cornelis Lütgebaucks[a], Halil I. Okur, Alex G. F. de Beer and Sylvie Roke*

Laboratory for fundamental BioPhotonics (LBP), Institute of Bioengineering (IBI), and Institute of Materials Science (IMX), School of Engineering (STI), and Lausanne Centre for Ultrafast Science (LACUS), École Polytechnique Fédérale de Lausanne (EPFL), CH-1015 Lausanne, Switzerland

[a] These two authors contributed equally

** Corresponding author: sylvie.roke@epfl.ch*

This PDF file includes:

Supplementary Text

S1. Lipids – Structure and liposome characterization

Lipids used in this study are: 1,2-dioleoyl-*sn*-glycero-3-phosphocholine (DOPC), 1,2-dipalmitoyl-*sn*-glycero-3-phosphocholine (DPPC), 1,2-dioleoyl-*sn*-glycero-3-phospho-L-serine (sodium salt) (DOPS), 1,2-dipalmitoyl-sn-glycero-3-phospho-L-serine (sodium salt) (DPPS), 1,2-dipalmitoyl-*sn*-glycero-3-phosphate (sodium salt) (DPPA), 1,2-dipalmitoyl-sn-glycero-3-phosphoethanolamine (DPPE), d_{62}-1,2-dipalmitoyl-sn-glycero-3-phospho-L-serine (sodium salt) (d_{62}-DPPS), and d_{66}-1,2-dioleoyl-*sn*-glycero-3-phosphocholine (d_{66}-DOPC). The chemical structures of the used lipids are presented in Fig. S1 and the liposome characterization is given in Table S1.

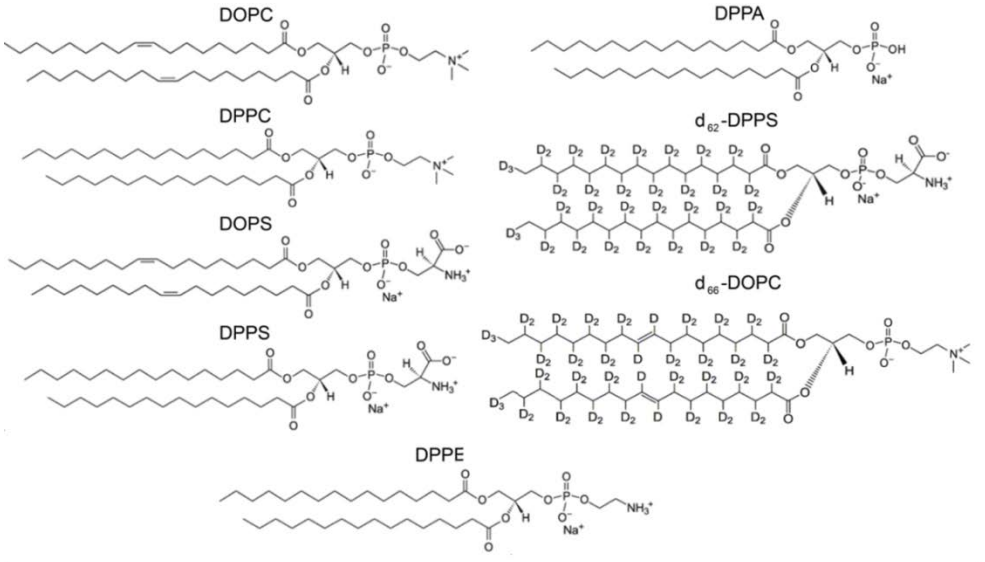

Figure S1: Chemical structures of the used phospholipids.

Table S1. The results of dynamic light scattering and zeta potential measurements. Standard deviations from the mean of three measurement are given in parenthesis.

Sample	Hydrodynamic diameter (nm)	Zeta potential (mV)
DPPS	98.4(0.5)	-45(1)
DOPC	94.0 (0.3)	-6(1)
DPPC	96.0 (0.3)	-4(1)
d_{66}-DOPC:DPPS	90.4(0.4)	-42(1)
DOPC:d_{62}-DPPS	69.8(0.3)	-43(1)
DOPC:DPPS	95.3(0.3)	-43(1)
d_{66}-DOPC:DPPA	99.2(0.5)	-36(1)
DOPS:DPPS	73.0(0.3)	-52(2)

Vibrational sum frequency spectra were measured using the setup for sum frequency generation experiments described in Ref. [1-3]. An 800 nm regeneratively amplified Ti:sapphire system (Spitfire Pro, Spectra physics) seeded with an 80 MHz 800 nm oscillator (Integral 50, Femtolasers) was operated at a 1 kHz repetition rate to pump a commercial OPG/OPA/DPG system (HE-TOPAS-C, Light Conversion), which was used to generate IR pulses. The visible beam was split off directly from the amplifier, and spectrally shaped with a home-built pulse shaper. The angle between the 10 µJ visible (VIS) beam (800 nm, FWHM 15 cm^{-1}) and the 6 µJ IR beam (9700 nm or 3200 nm, FWHM 160 cm^{-1}) was 20° (as measured in air). The focused laser beams were overlapped in a sample cuvette with a path length of 200 µm. At a scattering angle of 55°, the scattered SF light was collimated using a plano-convex lens (f=15 mm, Thorlabs LA1540-B) and passed through two short wave pass filters (3rd Millenium, 3RD770SP). The SF light was spectrally dispersed with a monochromator (Acton, SpectraPro 2300i) and detected with an intensified CCD camera (Princeton Instruments, PI-Max3) using a gate width of 10 ns. The acquisition time for a single spectrum was 10-20 min for PO stretch modes and 40 min for CH stretch modes for liposomes. A Glan-Taylor prism (Thorlabs, GT15-B), a half-wave plate (EKSMA, 460-4215) and a polarizing beam splitter cube (CVI, PBS-800-050) and two BaF_2 wire grid polarizers (Thorlabs, WP25H-B) were used to control the polarization of the SFG, VIS and IR beams respectively. The SFG, and VIS beams were polarized in the vertical (S) direction, and the IR beam was polarized in the horizontal plane (P), leading to the polarization combination $S_{out}S_{in}P_{in}$. The recorded intensity was baseline subtracted and normalized to the SFG spectrum of a gold mirror in $P_{out}P_{in}P_{in}$ polarization that was recorded before each measurement.

Second harmonic scattering measurements were performed, as previously described in detail [4], using 190 fs laser pulses at 1028 nm with a 200 kHz repetition rate. The input polarization is controlled by a Glan-Taylor polarizer (GT10-B, Thorlabs) and a zero-order half wave plate (WPH05M-1030). The filtered (FEL0750, Thorlabs) input pulses with a pulse energy of 0.3 µJ (incident laser power P = 60 mW) were focused into a cylindrical glass sample cell (4.2 mm inner diameter) with a waist diameter of ~32 µm and a Rayleigh length of 3.2 mm. The scattered SH light was collected and collimated with a plano-convex lens (f = 5 cm), polarization analyzed (GT10-A, Thorlabs), filtered, (ET525/50, Chroma) and finally focused into a gated PMT (H7421-40, Hamamatsu). Data points for scattering patterns were acquired in steps of 5° from -90° to 90° and an acceptance angle of 3.4°. Typically, measurements settings were 20 x 2 s acquisition time and a gate width of 10 ns. To correct for incoherent hyper Rayleigh scattering from the aqueous phase, both the SHS response from the liposome solution and the SHS response from the solution without liposomes are detected under the same conditions. The SHS intensity from the solution is then subtracted from the SHS intensity from the liposome solution. The obtained difference is then normalized to the isotropic SSS signal of pure water, so that we correct for any form of aberration

due to differences in the beam profile and obtain a value that can be compared to any other measurement done in the same procedure. The reproducibility of the SHS measurements is 1-2 % (for aqueous solutions) and 5-6 % for the used liposome solutions. The latter number reflects the uncertainty in the reproducibility of the preparation of the liposomes.

$$\mathrm{S}(\theta) = \left[\frac{I(\theta)_{SHS,liposomes,PPP} - I(\theta)_{SHS,solution,PPP}}{I(\theta)_{SHS,water,SSS}} \right] \quad (1)$$

All measurements were performed at 25 °C.

S2. Normalization and correction for the difference in size distribution

In order to get a comparable value for the scattered SHS or SFS light from different samples we normalized the above measured value in Eq. (1) by the number of droplets (N_d) or liposomes (N_{lip}), obtainable from the amount of lipid used and the DLS distribution and correct for the difference in the radius (R).

For a *monodisperse* solution of droplets or liposomes that are smaller than ~200 nm in radius the total scattered signal (*S*) from a solution with N_p particles that each scatter an intensity $I(\theta)$ scales as follows [5]:

$$S(\theta) = I(\theta)N_p \propto \alpha(\theta)N_p R^6 \quad (2)$$

The factor α contains all the information about the surface response per droplet / liposome, independent of its size. Thus, if we want to compare the lipid or water response per droplet or liposome we have to compute the following:

$$\alpha(\theta) = \frac{\mathrm{S}(\theta)}{N_p R^6} = I_{norm}(\theta, R)\,, \quad (3)$$

which is what we have used in this work, and plot on the y-axis in Fig. 1A. Note that for the SFS data we plot the measured spectrum (I_{SF}/I_{IR}) and then use the procedure outlined in S5 to compute the average asymmetry per liposome in lipid number density using the fitted amplitudes of the symmetric P-O stretch and the symmetric CH_3 stretch mode as input. For both the SHS and SFS experiments we correct for polydispersity by replacing the radius *R* in Eq. (3) with an effective radius (R_{eff}). The procedure to calculate R_{eff} is described below.

S3. Calculation of an effective radius

Since all particles contribute in the same way to the overall intensity of any light scattering experiment, we can use the DLS data to compute an effective radius that can be used for SHS and SFS experiments on polydisperse samples. DLS uses the temporal autocorrelation of scattered light to measure an intensity-weighted particle size distribution histogram. The output of such a measurement is a (normalized) distribution *D(R)*, which we will use here to correct the SHS and SFS signal for variations in the droplet / liposome size distribution, which affects both the scattered intensity per scatterer and the number of scatterers. In other words, we want to replace the total DLS intensity from a polydisperse distribution $\sum_i I(R_i)$ by an intensity $I_{norm}(\theta,R_{eff})$ from a 'monodisperse' solution. The obtained effective radius can then be used to normalize the SH intensity according to Eq. (3). In this way, we exclude intensity differences based on different sample sizes and obtain the surface scattering contribution $\alpha(\theta)$, which contains information about surface packing, hydration and orientation of water molecules of a single scatterer. Explicitly we have from Eq. (3):

$$\alpha(\theta) = \frac{\sum_i I_i(\theta)}{N_p R^6} = \frac{S(\theta)}{N_p R_{eff}^6} = I_{norm}(\theta) \qquad (4)$$

In the RGD limit, which is applicable here[6], the intensity of scattered light in a DLS measurement also scales with R^6, so that:

$$D(R) = \frac{P(R)R^6}{\int P(R)R^6 dR} \qquad (5)$$

The particle size distribution *P(R)* is a normalized probability distribution, such that $\int P(R)dR = 1$.

We can calculate the particle size distribution from the DLS intensity-weighted distribution by:

$$P(R) = \frac{D(R)}{R^6} / \int \frac{D(R)}{R^6} dR \qquad (6)$$

Using the particle size distribution we then calculate the effective radius for the liposomes using the following general expression:

$$R_{eff,lip} = \left[\frac{\int P(R)R^6 dR}{\int \frac{1}{2} P(R)(R^2 + (R-d)^2) dR} \right]^{1/4}, \qquad (7)$$

where the denominator takes into account that with changing radius the number of lipids per liposomes changes too (i.e. size and number density are related). For nanodroplets we have the following expression:

$$R_{eff,d} = \left[\frac{\int P(R) R^6 dR}{\int P(R) R^3 dR} \right]^{1/3}, \quad (8)$$

where the denominator is now representing a sphere rather than a hollow shell.

S4. SFS spectral fitting

The SFS signal (S) can be described by the following Lorentzian line shape expression[7]:

$$S_{SFS}(\theta, \omega) \propto \left| A_{NR}(\theta) f(\omega) e^{i\varphi_{NR}} + \sum_i \frac{A_i(\theta)\gamma_i}{\omega - \omega_i + i\gamma_i} \right|^2, \quad (9)$$

where $A_{NR}(\theta)$ is the amplitude and $f(\omega)$ is the spectral shape of a weakly dispersive ('non-resonant') background, φ_{NR} is the phase of the background signal relative to that of the resonant signal, $A_i(\theta)$ is the amplitude of the ith vibrational mode with the resonance frequency ω_i and linewidth γ_i. The strength of the vibrational mode is proportional to A_i ($\omega = \omega_i$). The SFS spectra (I_{SF}/I_{IR}) were fitted using Eq. 9, employing IGOR Pro 6 (WaveMetrics) and using Levenberg-Marquardt iterations. The fitted parameters for the SFS spectra are shown in Table S2 and S3. The SFS intensity in the s-PO_2^- stretch region in the SPS polarization combination was too low to reliably fit for all the samples.

The SFS spectra that do not show any detectable features are fitted with a 3rd order polynomial.

Table S2: Fitted frequency, amplitude and linewidth for the SFS spectrum in the C-H and P-O stretch region of d_{66}-DOPC:DPPS liposomes.

mode	ω_i (cm^{-1})	Υ_i (cm^{-1})	A_i
r^+	2868	20	0.15
d^+_{FR}	2926	16	0.11
r^-	2968	20	0.14
d^-	2906	20	0.02

Table S3: Fitted frequency, amplitude and linewidth for the SFS spectra in the P-O stretch.

Sample		DOPC:DPPS		DPPC on oil		DEPC on oil	DOPS:DPPS
Polarization		SSP	PPP	SSP	PPP	SSP	SSP
ss PO_2^-	A_i	1.13	1	1.85	1	1	1
	ω_i (cm^{-1})	1079	1079	1099	1096	1085	1083
	Υ_i (cm^{-1})	17	17	10	13	20	13
ss C-O-P	A_i			1.31	0.93		
	ω_i (cm^{-1})			1072	1066		
	Υ_i (cm^{-1})			20	12		

S5. Calculation of the orientational distribution of phosphate groups

The orientational analysis to calculate the ratio of SFS amplitudes in SSP and PPP polarization combinations of the s-PO_2^- vibration is adapted from our procedure published earlier[8,9] based on the Rayleigh-Gans-Debye approximation in combination with nonlinear light scattering theory. We use a tilt angle ϕ of the PO_2^- group with respect to the surface normal and a twist angle ψ of the PO_2^- group around its molecular axis. This results in the following relations[10] between the surface second-order susceptibility ($\boldsymbol{\chi}^{(2)}$) and molecular hyperpolarizability ($\boldsymbol{\beta}^{(2)}$) tensor elements:

$$\chi_{xxz}^{(2)} = \chi_{yyz}^{(2)} = \frac{1}{2}N(\beta_{aac}^{(2)}cos^2\psi + \beta_{bbc}^{(2)}sin^2\psi + \beta_{ccc}^{(2)})cos\phi + \frac{1}{2}N(\beta_{aac}^{(2)}sin^2\psi + \beta_{bbc}^{(2)}cos^2\psi - \beta_{ccc}^{(2)})cos^3\phi$$

$$\chi_{zzz}^{(2)} = N\left(\beta_{aac}^{(2)}sin^2\psi + \beta_{bbc}^{(2)}cos^2\psi\right)cos\phi - N(\beta_{aac}^{(2)}sin^2\psi + \beta_{bbc}^{(2)}cos^2\psi - \beta_{ccc}^{(2)})cos^3\phi \quad (10)$$

with N the surface density of PO_2^- groups. We assume that the droplet/liposome interface is azimuthally isotropic. The values of the second-order hyperopolarizability tensor elements were taken from Ref.[10].

S6. Calculation of the degree of asymmetry based on geometrical arguments

The number of lipids per leaflet can be calculated assuming that the liposomes have a spherical shape. We assume that each lipid headgroup occupies a constant area, *a*, which is the same at the inner and outer leaflets.[11] Then we get for the respective number difference (ΔN) between the outer leaflet and inner leaflet: $\Delta N = \frac{4\pi((R^2-(R-d)^2)}{a}$. ΔN can be expressed as a percentage of the total lipid number density per liposome (N_{tot}), which is given by $N_{tot} = \frac{4\pi((R^2+(R-d)^2)}{a}$. Here, *R* is the outer radius of the liposome and *d* is the membrane thickness, for which we take d ~ 5 nm.

S7. Calculation of the degree of asymmetry from the SFS data

For a monodisperse solution, the number densities (N_d) of nanodroplets can be calculated by dividing the volume concentration of oil in the sample (V_{oil}) by the volume of one droplet with radius R_d:

$$N_d = \frac{V_{oil}}{\frac{4}{3}\pi R_d^3}. \quad (11)$$

For liposomes we have a spherical bilayer rather than a sphere with radius R_{lip} and thickness d and lipid volume concentration V_{lip}, so that the number density of liposomes is different:

$$N_{lip} = \frac{V_{lip}}{\frac{4}{3}\pi(R_{lip}^3 - (R_{lip}-d)^3)}. \quad (12)$$

For the calculation of the number density of liposomes we use d = 5 nm [12].

To extract the degree of asymmetry for a certain vibrational mode accounting for polydispersity, we fit the obtained spectra according to Eq. 9 and use the obtained amplitude $A_i(\theta)$ in the expression for α (Eq. 4):

$$\alpha_{lip,i}(\theta, R_{eff,lip}) = \frac{|A_i(\theta)|^2}{N_{lip} R_{eff,lip}^6} \quad (13)$$

This value is now independent of liposomes size, has been corrected for polydispersity and can be compared to other samples. For droplets we obtain the same expression. The parameters of the emulsions and liposomes and calculated degree of asymmetry are shown in Tables S4 and S5.

Table S4: Calculation of the degree of transmembrane asymmetry for d_{66}-DOPC:DPPS liposomes, using a DPPC monolayer on an oil droplet with known lipid density as a reference.

Sample	DPPC on $C_{16}D_{34}$ (droplets)	d_{66}-DOPC:DPPS (liposomes)
R_{eff}, nm	97.6	41.4
concentration	2 vol%	5 mg/ml
A_i, s-CH_3 mode	3.87	0.15
$\frac{n_{sample}}{n_d}$, s-CH_3 mode	1	0.16

Table S5: Calculation of the degree of head group orientation asymmetry for DOPC:DPPS and DOPS:DPPS liposomes, using a DPPC monolayer on an oil droplet with known lipid density as a reference.

Sample	R_{eff}, nm	$\frac{n_{sample}}{n_d}$, s-PO_2^- mode
DOPC:DPPS	33	0.95
dDOPC:DPPS	44	0.88
DOPS:DPPS	33	0.92

S8. Additional SFS experiments

In addition to the data shown in the manuscript, we tested all DO/DP tail combinations of PC:PS mixed liposomes. The SFS spectrum of DOPC:DPPS and DOPS:DPPC (Figure S2 and Figure 4) along with DPPC:DPPS and DOPC:DOPS (Figure S2) mixed liposomes were measured. Only the DOPC:DPPS liposomes generate a detectable SFS response in the phosphate spectral region.

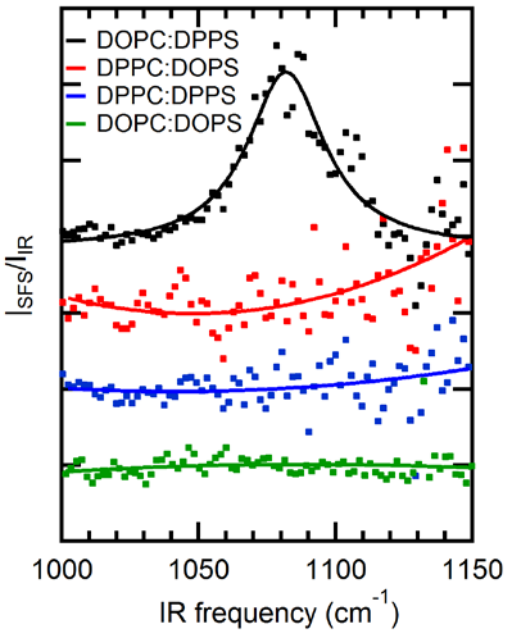

Figure S2. SFS spectra of mixtures of PC and PS lipids with different combinations of fatty acid tails: DOPC:DPPS (black), DPPC:DOPS (red), DPPC:DPPS (blue) and DOPC:DOPS (green). The SFS data are offset vertically for clarity.

References

(1) de Aguiar, H. B.; Samson, J.-S.; Roke, S. *Chem. Phys. Lett.* **2011**, *512*, 76.

(2) de Aguiar, H. B.; Scheu, R.; Jena, K. C.; de Beer, A. G. F.; Roke, S. *Phys. Chem. Chem. Phys.* **2012**, *14*, 6826.

(3) Scheu, R.; Chen, Y.; Subinya, M.; Roke, S. *J. Am. Chem. Soc.* **2013**, *135*, 19330.

(4) Gomopoulos, N.; Luetgebaucks, C.; Sun, Q.; Roke, S. *Opt. Express* **2013**, *21*, 815.

(5) de Beer, A. G. F.; Roke, S. *Phys. Rev. B* **2009**, *79*, 155420.

(6) de Beer, A. G. F.; Roke, S. *Phys. Rev. B* **2007**, *75*, 245438.

(7) de Aguiar, H. B.; Strader, M. L.; de Beer, A. G. F.; Roke, S. *J Phys Chem B* **2011**, *115*, 2970.

(8) Chen, Y.; Jena, K. C.; Lütgebaucks, C.; Okur, H. I.; Roke, S. *Nano Lett.* **2015**, *15*, 5558.

(9) de Beer, A. G. F.; Roke, S. *J. Chem. Phys.* **2010**, *132*, 234702.

(10) Casillas-Ituarte, N. N.; Chen, X.; Castada, H.; Allen, H. C. *J Phys Chem B* **2010**, *114*, 9485.

(11) Israelachvili, J. N. *Intermolecular and surface forces*; Academic Press; New York, 1991.

(12) Gramse, G.; Dols-Perez, A.; Edwards, M. A.; Fumagalli, L.; Gomila, G. *Biophys. J.* **2013**, *104*, 1257.